Phase behavior in the reentrant-nematic region of chiral frustrated smectic liquid crystals

G. S. Iannacchione and C. W. Garland
Department of Chemistry and Center for Material Science and Engineering, Massachusetts Institute of Technology, Cambridge, Massachusetts 02139

J. Mieczkowski and E. Gorecka
Department of Chemistry, Warsaw University, 02-089 Warsaw, Poland
(Received 16 October 1997; revised manuscript received 23 February 1998)

A high-resolution ac calorimetric study has been carried out on two homologous polar liquid crystals with aromatic cores containing three phenyl groups and a flexible chiral linking group. The expected smectic polymorphism occurs, and there are several prominent thermal features in the nematic range between smectic-A_d and smectic-$\tilde{C}$ phases. It is suggested on the basis of characteristic thermal signatures, helical pitch variations, and optical textures that a twist-grain-boundary phase and chiral line liquids (N_L^*) exist as well as twisted nematic liquid crystals (N^*) with other kinds of short-range order. [S1063-651X(98)03607-1]

PACS number(s): 64.70.Md, 65.20.+w, 61.30.−v

I. INTRODUCTION

Smectic polymorphism and reentrant nematic phases are well known in ''frustrated'' smectic liquid crystals exhibiting long (three-ring) aromatic cores and a polar end group [1]. The best experimentally studied systems of this type are alkoxybenzoyloxy cyanostilbenes (T7 and T8) [2] and mixtures of alkoxyphenyl-nitrobenzoyloxy benzoates ($DB_8ONO_2+DB_{10}ONO_2$) [3,4]. The theory of such systems has been developed along two different lines [5,6], both of which involve a competition between two length scales. One of these lengths is the molecular length L and the other is the polarization periodicity reflected in the layer spacing d for the partial bilayer smectic-A_d (SmA_d) phase ($d\sim 1.2$ L in the systems studied here).

It is also well known that chirality promotes twisted phases [7] such as the blue phases (BP's), cholesteric (N^*), and twist-grain-boundary (TGB) phases. Theory has predicted both TGB_A and TGB_C phases [8–10]; the most extensive experimental studies of TGB_A and TGB_C are reported in Refs. [11, 12] and Refs. [13, 14], respectively.

Recently, studies have been carried out on the mesogenic phenyl butyrates *R*-(+)-4-[(E)-2-(4-alkoxyphenyl)-1-diazenoxid]-phenyl-3-(4-nitrophenyl)-butanoate, with the structural formula

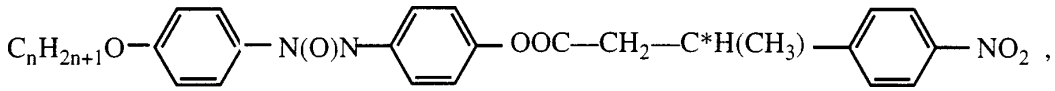

for homologs with $n=11-17$ [15,16]. This compound was denoted *n*AZY in Ref. [15], but we prefer the more structurally related abbreviation *n*OPBNO$_2$ and will refer to it by this name. Since this polar compound contains a three-ring aromatic core with a chiral linking group, it should exhibit phase aspects of both frustrated smectics and chiral materials. The partial phase diagram shown in Fig. 1 exhibits the expected smectic polymorphism, and previous DSC studies of the $n=14-17$ homologs [16] indicated a prominent thermal feature in the nematic region, which was tentatively ascribed to a transition similar to the nematic N_d-nematic N_1 transition reported in Ref. [17]. The present investigation involves a high-resolution ac calorimetric study of the *R*-enantiomers of 14OPBNO$_2$ ($M=611.74$ g mol^{-1}) and 15OPBNO$_2$ ($M=625.77$ g mol^{-1}), with special emphasis on the nematic region. One first-order transition and three nontransitional thermal features were observed in this region, as described in Sec. II. A discussion comparing the new results with those for systems with known TGB phases and proposing several N^* regions with differing short-range order is given in Sec. III. It should be noted that the pitch in most of the nematic range for these $n=14$ and 15 compounds is found to be less than 0.2 μm (ultraviolet region), which indicates a substantial chirality (twisting tendency).

II. CALORIMETRIC AND OPTICAL RESULTS

The synthesis and purification of the investigated phenyl butyrates (as described in Ref. [15]), optical observations of textures and helical pitch, and DSC scans were carried out at the University of Warsaw. The heat capacity data given for the $n=14$ and 15 homologs in Figs. 2 and 3 were obtained at MIT with a high-resolution ac calorimeter, operated over a range of frequency from $2\omega_0$ to $\omega_0/8$, where $\omega_0=2\pi f_0=0.196$ s^{-1}. A small mass (~ 30 mg) of liquid crystal was cold-weld sealed into a thin silver cell, and the temperature was scanned slowly (0.1–0.2 K h^{-1}) to ensure thermody-

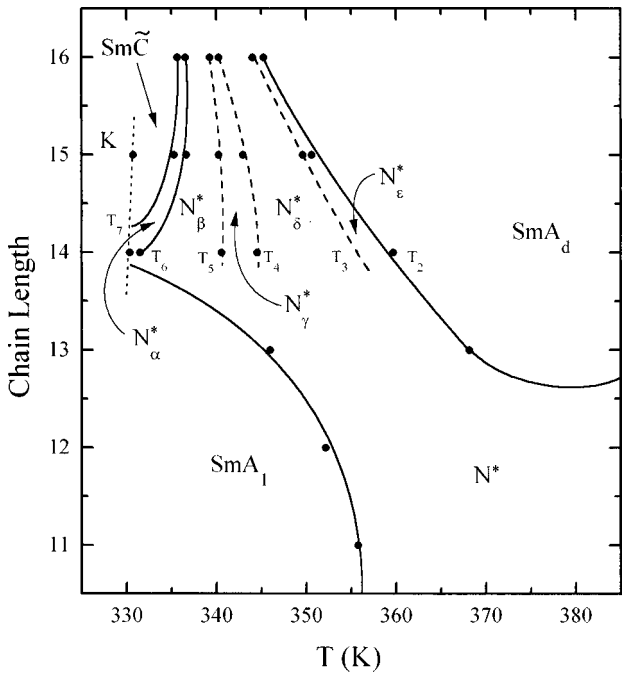

FIG. 1. Partial phase diagram for the chiral homologous series nOPBNO$_2$. Data for $n=14-16$ are based on the C_p results in Sec. II. All other data are taken from Ref. [16], which gives full diagrams for the R-enantiomer and racemic mixtures. The vertical short dashed line shows where freezing occurs on slow cooling runs. The long dashed lines represent nontransitional evolutions of short-range order. Further information about ''transitions'' T_2-T_7 involving twisted nematics N^*_α-N^*_ε is given in Table I.

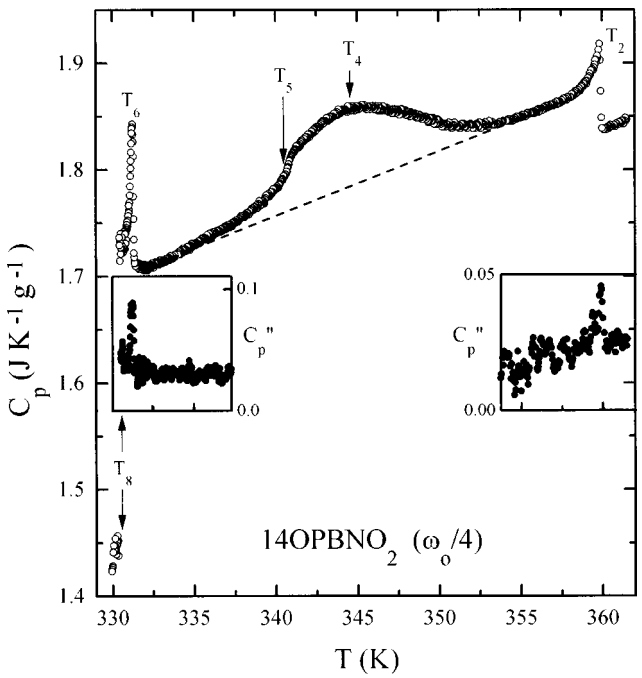

FIG. 2. Heat capacity C_p for 14OPBNO$_2$ obtained on a cooling run with a scan rate of -0.1 K h^{-1}. The labels T_n correspond to features shown in Fig. 3 and listed in Table I. Two insets of C_p'' behavior support the assignment that T_2 and T_6 are first-order phase transitions.

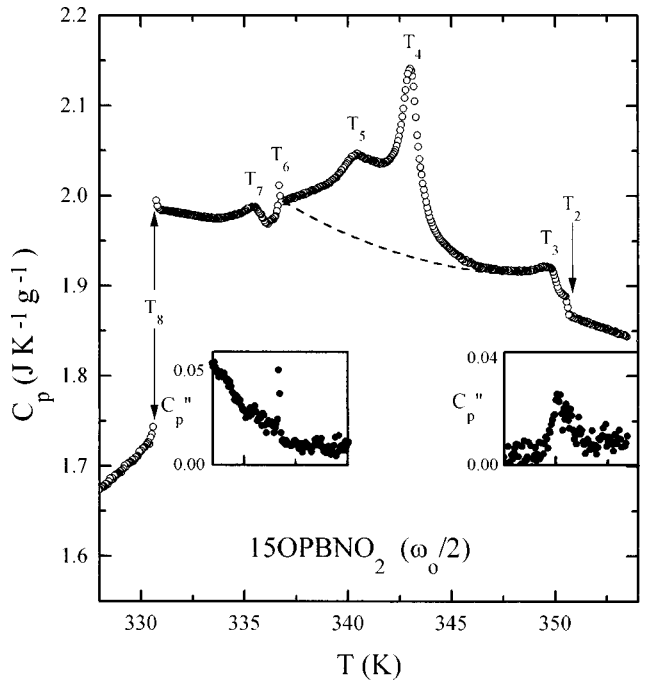

FIG. 3. Heat capacity C_p for 15OPBNO$_2$ for a cooling run with a scan rate of -0.15 K h^{-1}. The labels T_n correspond to those in Fig. 2 and Table I. The insets show C_p'' peaks associated with two-phase coexistence at the first-order T_2 and T_6 transitions. See the text concerning a frequency-dependent behavior of C_p'' for temperatures below T_6.

namic equilibrium for the mesogenic phases. No appreciable drift in the position of C_p peaks was observed over a period of eight weeks. The calorimeter and the equations for analyzing the observed T_{ac} response to the $P_{ac}=P_0\exp(i\omega t)$ heat input are described elsewhere [18,19]. The 14OPBNO$_2$ data in Fig. 2 were obtained at $\omega_0/4$ (7.8 mHz) and the 15OPBNO$_2$ data in Fig. 3 at $\omega_0/2$. In both cases, these are static values in one-phase regions since C_p values obtained at lower frequencies agreed well with those shown.

Also displayed in Figs. 2 and 3 are insets indicating the typical anomalies in the imaginary component C_p'', related to phase shifts ϕ between T_{ac} and P_{ac} seen at first-order transitions where there is two-phase coexistence [18,20]. In other regions, C_p'' is essentially independent of T and very small (~ 0.003 J K^{-1} g^{-1}) except for an unusual smooth rise in C_p'' for 15OPBNO$_2$ on cooling from ~ 338 K to the freezing point at 330.7 K. Over this ~ 7 K range, C_p'' increases by 0.061 J K^{-1} g^{-1} (from ~ 0.006 to 0.067 J K^{-1}g^{-1}) for $\omega_0/2$. This effect is frequency dependent: the increase in C_p'' is 0.115 J K^{-1} g^{-1} at $2\omega_0$ but disappears at $\omega_0/6$ and $\omega_0/8$. Thus, this C_p'' effect is due to sluggish dynamics in this temperature region and not to two-phase coexistence [19].

The thermal features shown in Figs. 2 and 3 are listed in Table I together with melting temperatures of the crystal phase on heating and previously reported DSC values for the high-temperature isotropic (I)–smectic-A_d (SmA_d) transitions. Note that several of the transitions are monotropic since there is a considerable difference between the freezing and melting temperatures. In the case of 14OPBNO$_2$, the sample was quenched to 330.5 K and a heating run was immediately begun prior to any freezing. This was not done

TABLE I. Transition temperatures (K) and enthalpies (J g^{-1}) for chiral nOPBNO$_2$. T_3-T_5 denote three nonsingular (rounded) C_p features that do not correspond to thermodynamic phase transitions. m denotes that the feature is monotropic.

Phase	Proposed structure	Proposed transition	Order		$n=14$	$n=15$
I	I					
		I-SmA_d	1st	T_1 [16]	~396	~399
				ΔH_1 [16]	5.4 DSC	7.3 DSC
SmA_d	SmA_d					
		SmA_d-N_d^*	1st	T_2	359.68	350.60
				ΔH_2 [16]	0.08 DSC	0.06 DSC
N_ε^*	N_d^*					
		(N_d^*-N^*)	non	T_3	?	349.6
N_δ^*	N^*					
		(N^*-N_{LA}^*)	non	T_4	344.55	342.94
N_γ^*	N_{LA}^*					
		(N_{LA}^*-N_{LC}^*)	non	T_5	340.57, m	340.25
N_β^*	N_{LC}^*					
		N_{LC}^*-TGB$_C$	1st	T_6	331.22, m	336.66, m
				ΔH_6 [16]	0.19 DSC	0.26 DSC
N_α^*	TGB$_C$					
		TGB$_C$-Sm$\tilde{C}$	1st?	T_7		335.3, m
				ΔH_7		~0.05 DSC
Sm$\tilde{C}$	Sm$\tilde{C}$					
		freeze to K	1st	T_8	330.35[a]	330.73[b]
K	K					
		K melt			344.05[a]	339.75[b]

[a]TGB$_C$ freezes into K; K melts into N_{LA}^*.

[b]Sm$\tilde{C}$ freezes into K at a scan-rate-dependent temperature; K melts into N_{LC}^*.

for 15OPBNO$_2$, and only cooling run data are available below 340 K. The symbols N_α^* to N_ε^* are used in Fig. 1 and Table I to denote the various twisted phases observed in the reentrant nematic region. The low-temperature smectic phase that we assign as Sm$\tilde{C}$ is denoted as SmX in Ref. [16], where on the basis of preliminary x-ray powder patterns it was shown to be either a weakly tilted Sm$\tilde{C}$ phase or an incommensurate orthogonal smectic mesophase. A discussion of possible structures for $N_\alpha^*-N_\varepsilon^*$ in terms of twist-grain-boundary, chiral line liquids N_L^*, and twisted nematic N^* phases is given in Sec. III.

The first-order character of the transitions at T_2 and T_6 is very clear. In both compounds there are characteristic low-frequency C_p'' peaks that arise from ac phase-shift anomalies and indicate two-phase coexistence [20]. The width of the coexistence region at T_2 is ~0.8 K for $n=14$ and ~1.0 K for $n=15$, while the coexistence width at T_6 is 0.35 K for $n=14$ and 0.23 K for $n=15$. Furthermore, there is a substantial hysteresis of 0.5 K at the T_2 transition for $n=15$. The T_6 hysteresis is very small for the $n=14$ compound (0.01 K) and was not investigated for $n=15$. Estimated values of the latent heats ΔH_2 and ΔH_6 given in Table I are taken to be the total DSC enthalpies reported in Ref. [16] for these transitions.

The nature of the T_7 thermal feature observed in 15OPBNO$_2$ is uncertain. If it were found by structural studies to be a TGB$_C$-Sm$\tilde{C}$ transition, one would expect it to be first order like the analogous TGB$_C$-SmC^* transition [14]. However, in the latter case the variation of C_p(ac) is very small and the latent effect associated with this transition is observed only by nonadiabatic scanning calorimetry, which was not used in the present study. Both the C_p(ac) and the new DSC runs show a rounded T_7 feature for 15OPBNO$_2$, and there are no obvious anomalies in the phase shift ϕ signaling two-phase coexistence at T_7. However, such ϕ anomalies are subtle at the TGB$_C$-SmC^* transition [14]. We have tentatively assumed a first-order character and list the DSC area in Table I as the latent heat ΔH_7. This value of ~0.05 J g^{-1} agrees well with latent heats of 0.052 and 0.126 J g^{-1} reported for two TGB$_C$-SmC^* transitions [14]. Note that a ''T_7 transition'' is missing for 14OPBNO$_2$ due to the sample freezing just below T_6.

The features labeled T_3, T_4, and T_5 denote nontransitional evolutions of the short-range order in the nematic phase. These three features are obvious from rounded C_p peaks observed for 15OPBNO$_2$, but the T_3 feature is not obvious for 14OPBNO$_2$ and the T_5 feature is seen as a rounded step (see Fig. 2). None of the T_3, T_4, T_5 features exhibit hysteresis, there are no C_p'' peaks or other C_p'' anomalies associated with these features, and the shapes of the C_p peaks do not correspond to either first-order behavior or singular second-order behavior.

Although it is difficult to make a precise evaluation of the excess heat capacity ΔC_p due to ambiguities in

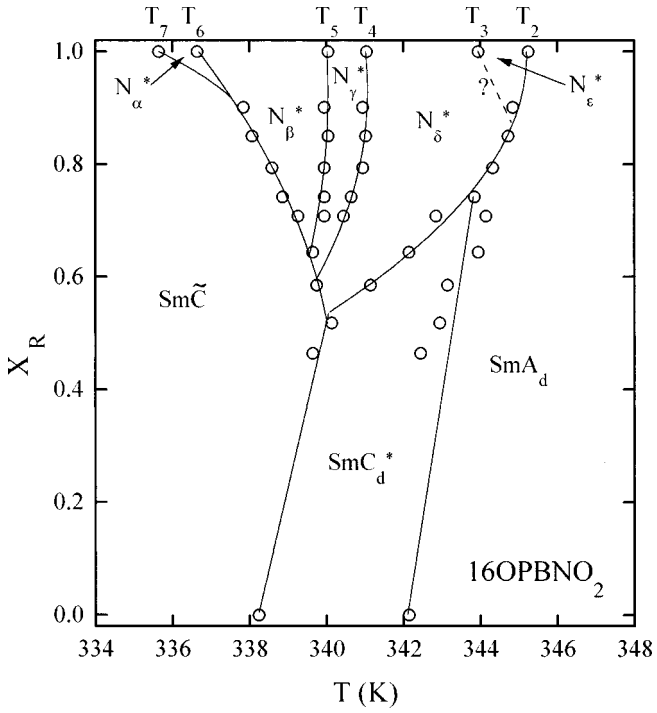

FIG. 4. Phase diagram for mixtures of R-16OPBNO$_2$ and its racemate obtained from DSC scans made at 1 K min^{-1}. X_R is the mole fraction of the chiral enantiomer.

C_p(background), an estimate has been made of the excess enthalpy δH associated with the combined T_4 and T_5 features using

$$\delta H = \int \Delta C_p dT, \tag{1}$$

where the excess heat capacity is $\Delta C_p = C_p$(observed) $- C_p$(background). The C_p(background) values are indicated by the dashed lines in Figs. 2 and 3. The choice of C_p(background) is especially difficult for 15OPBNO$_2$ since the first-order T_6 transition is much closer to T_4 ($\sim$6.3 K compared to $\sim$13.3 K for 14OPBNO$_2$). The resulting enthalpies δH are 0.65 J g^{-1} for 14OPBNO$_2$ and $\sim$0.61 J g^{-1} as an estimated *lower bound* for 15OPBNO$_2$.

DSC scans carried out at Warsaw University confirm qualitatively most of the thermal features obtained with ac calorimetry. For the $n=15$ and 16 compounds, better DSC resolution was obtained than that shown in Ref. [16] and six peaks corresponding to T_2-T_7 were observed above the freezing temperature. For the $n=14$ compound, DSC and ac calorimetry agree in that neither shows a peak at T_3 and both show freezing occurs just below T_6 (even at a DSC scan rate of 5 K/min). The DSC for $n=14$ does not show the step feature in C_p at T_5. DSC transition temperatures obtained on heating are systematically 1.1 K higher than those determined with ac calorimetry, due in part to rapid DSC scan rates and in part to absolute temperature calibrations. The $n=16$ points in Fig. 1 have been shifted by 1.1 K to permit a better correspondence with the present data for $n=14$ and 15. It should be noted that DSC scans do not allow one to distinguish first-order and second-order transitions from each other or from nontransitional thermal features. Such distinctions require high-resolution data obtained at slow scan rates.

An additional DSC study was undertaken on mixtures of chiral R-16OPBNO$_2$ and its racemate, and the resulting phase diagram is given in Fig. 4. As the chiral mole fraction X_R is decreased, the N^*_α and N^*_ε phases disappear and the phase sequence becomes SmA_d-N^*_δ-N^*_γ-N^*_β-Sm$\tilde{C}$ at $X_R = 0.8$. Note that the location of the T_3 line is uncertain since DSC scans of mixtures do not resolve the small T_3 feature on the low-temperature side of an asymmetric T_2 peak. As the chirality is further reduced, the remaining N^* phase regions decrease and disappear and a SmC^*_d tilted bilayer phase appears. The DSC enthalpy for the combined T_4+T_5 features decreases from 0.45 J g^{-1} at $X_R=0.9$ to 0.07 J g^{-1} at $X_R = 0.7$.

Optical measurements made at Warsaw University show that the helical pitch for the $n=14$ and 15 homologs in the N^*_β, N^*_γ, and N^*_δ phases is less than 0.2 μm. As the temperature approaches the SmA_d and Sm$\tilde{C}$ boundaries, the helical pitch increases rapidly ($|dP/dT| \sim 0.13$ μm/K) to give selective light reflections in the visible. Such a small pitch in reentrant N^*_β-N^*_δ nematic phases confirms the substantial chirality of these compounds. Also the width of the region of rapid increase in pitch on heating 15OPBNO$_2$ near the SmA_d boundary is 1.0 K, which exactly agrees with the width of the calorimetric region labeled N^*_ε, and the width of the region of rapid increase of pitch on cooling near the Sm$\tilde{C}$ boundary is 0.75–1.7 K, which compares well to the N^*_α range of 1.36 K from calorimetry.

In the nematic region from T_3 to T_6, where Fig. 1 indicates the presence of N^*_β, N^*_γ, and N^*_δ, smooth optical textures with a few oily streaks were observed, which are typical for chiral nematics with small helical pitch values. However, when the sample was heated or cooled rapidly, small square defects appeared in the N^*_γ temperature range between T_4 and T_5. These may be due to parabolic defects induced by small discontinuities in the helical pitch. At temperatures above T_2 and below T_7, fan textures were observed. In a freely suspended film (which should align the smectic layers parallel to the film surface), the SmA_d phase yielded a uniform homeotropic texture. The uniaxial untilted character of the SmA_d phase was also confirmed by conoscopic figures. In a freely suspended film of the low-temperature Sm$\tilde{C}$ phase, a uniform homeotropic texture was never observed and a weak fan texture was seen.

III. DISCUSSION

For the chiral nOPBNO$_2$ homologous series, the observed phase sequence is SmA_1-N^*-BP's-I for $n \leqslant 12$ and SmA_1-N^*_r-SmA_d-N^*-BP's-I for $n=13$, whereas the sequence is Sm$\tilde{C}$(=SmX)-N^*-SmA_d-I for $n=14$–16 [16]. Such smectic phase behavior is typical for long-core frustrated smectic liquid crystals with rigid linking groups between the phenyl rings [1–6] and occurs here where nOPBNO$_2$ has a flexible chiral linking group in the core. The discussion below will focus on the thermal behavior in the nematic region and will provide qualitative arguments in support of the structures proposed for the five phases

N^*_α-N^*_ε. The most likely assignments for these phases are TGB_C or $TGB_{\tilde{C}}$ (twist-grain-boundary phases with SmC or Sm$\tilde{C}$ blocks) for N^*_α, N^*_{LC} (chiral line liquid with *short-range* TGB_C or $TGB_{\tilde{C}}$ order) for N^*_β, N^*_{LA} (chiral line liquid with *short-range* TGB_A order) for N^*_γ, cholesteric N^* (twisted nematic with weak smectic fluctuations) for N^*_δ, and N^*_d (a weakly twisted nematic with dominant *short-range* SmA_d fluctuations) for N^*_ε. These proposed assignments are summarized in Table I. High-resolution x-ray studies on aligned single domain samples are needed to verify the presence of such TGB and chiral line liquid structures.

Based on the assignments proposed above, the transition at T_2 corresponds to SmA_d-N^*_d, where the nematic phase N^*_d is a long-pitch cholesteric with substantial short-range SmA_d fluctuations, which are expected to decrease and change in character on further cooling [21]. An example where such reentrant N_d behavior is established in analogous nonchiral frustrated smectic liquid crystals is given for octyloxybenzyloxy cyanostilbene (T8) in Ref. [2]. However, the presence of an asymmetric chiral center inside the aromatic core should strongly promote twisting, and the SmA_d fluctuations are in competition with this twisting tendency. Thus one expects N^*_d to evolve into N^*, which has a short pitch and weak smectic fluctuations. We assign this nontransitional change in nematic character to the thermal feature at T_3 in $15OPBNO_2$ and the associated significant change in pitch variation $|dP/dT|$. No thermal T_3 feature is visible in $14OPBNO_2$, but this is consistent with the smooth evolution of *short-range* SmA_d character to *short-range* SmC character in the nematic phase of T8 with only a single C_p(SmA_d-N) peak [2]. In the present materials, the asymmetry of the C_p peak associated with the first-order transition at T_2 is different from the usual shape of second-order N_r-SmA_d peaks. However, similar asymmetry (large N^* pretransitional wing and small SmA_d wing) has also been observed in mixtures of octylcyanobiphenyl (8CB) and a chiral compound [22], where it is ascribed to energy effects related to the development (or expulsion) of the cholesteric twist.

The most prominent C_p feature in the nematic region is the broad rounded peak at T_4. This has been assigned to the nontransitional development of *short-range* TGB character to create a chiral line liquid N^*_L. Such a chiral line liquid has been predicted theoretically [10] as the liquid crystal analogy of the Abrikosov flux vortex *liquid* in type-II superconductors. Since N^* and N^*_L have the same macroscopic symmetry, no thermodynamic transition should occur, and this is verified experimentally. Indeed, a large rounded C_p peak is a striking characteristic of the evolution of N^* into a chiral line liquid [12,14]. Furthermore, the C_p feature at T_4 does *not* correspond to behavior like that observed for N_d-N_1 transitions in nonchiral systems where the smectic fluctuations change from SmA_d-like to SmA_1-like [17]. It should also be noted that *racemic* $14OPBNO_2$ and $15OPBNO_2$ samples do not exhibit an analogous T_4 thermal feature in their reentrant N phases. Furthermore, the character of the small texture changes reported near T_4 in the chiral homologs [16] supports this assignment as a change in the short-range order. Thus the evidence for the appearance of a chiral line liquid at T_4 is indirect but very strong.

We suggest that the smectic blocks in the N^*_γ chiral line liquid may have SmA character and use the symbol N^*_{LA} to indicate this assignment. The thermal feature at T_5 is also experimentally shown to be a nontransition—no first-order coexistence or latent heat but $C_p(T)$ is not singular as it would be at a second-order transition. We suggest this feature may be due to a change in the character (tilt) of the smectic blocks that make up the short-range TGB order: N^*_{LA}-N^*_{LC}. The presence of short-range smectic-C order is supported by the presence of a stable SmC_d phase in Fig. 4 and in racemic $15OPBNO_2$ [16].

The observed rapid increase in pitch on cooling both $14OPBNO_2$ and $15OPBNO_2$ below T_6 corresponds very well with previously observed pitch variations in the TGB_C phase [13], and the first-order transition at T_6 is assigned as N^*_{LC}-TGB_C. This is analogous to the established N^*_{LC}-TGB_C transition in chiral compounds with a SmC^* phase [14]. We are assuming that parallel behavior can occur where the underlying smectic phase is Sm$\tilde{C}$ rather than SmC^*. However, in view of the very small ΔH_7 latent heat associated with the TGB_C-Sm$\tilde{C}$ transition in $15OPBNO_2$, the structure of the TGB_C phase must be very similar to that of the Sm$\tilde{C}$ phase. Thus it might be possible that this is a new $TGB_{\tilde{C}}$ phase where the smectic blocks have Sm$\tilde{C}$ structure. The argument against this is that such a structure would require grain boundaries with two types of more or less orthogonal dislocations, and the stability of these complex grain boundaries would be poor [23].

It is appropriate to mention two other possible phase sequences: (1) Sm$\tilde{C}$-TGB_C-TGB_A-N^*_L-N^*-N^*_d-SmA_d or (2) Sm$\tilde{C}$-TGB_{C1}-TGB_{C2}-N^*_L-N^*-N^*_d-SmA_d where there are two different TGB_C phases. There is theoretical [8,9] and experimental [11,13,14,24] support for each of these sequences. However, if the transition at T_5 were to correspond to a N^*_L-TGB transition it should be first order [12,14], whereas the present data show that the T_5 heat capacity peaks are nontransitional features. Furthermore, in the second case one would expect a rapidly varying and large pitch in both TGB_C phases [24], whereas we see a rapid increase in pitch on cooling only over a narrow temperature range corresponding to the single N^*_α region shown in Fig. 1.

It is useful to compare the widths and integrated enthalpies for the combined T_4 and T_5 peaks with published values for N^*-N^*_{LA} in TGB_A materials and N^*-N^*_{LC} in TGB_C materials. The ''width'' is $\sim$15 K and $\delta H = 0.65\ J\ g^{-1}$ for $14OPBNO_2$, and these values are $\sim$10 K and $\gtrsim 0.61\ J\ g^{-1}$ for $15OPBNO_2$. For N^*-N^*_{LA}, the widths range from 5 to 11 K and δH values vary from 0.8 to $1.8\ J\ g^{-1}$ [12,14]. For N^*-N^*_{LC}, the respective values are 5–8 K and $0.28–0.7\ J\ g^{-1}$ [14]. Thus the substantial amount of short-range ordering that occurs over a wide temperature range is comparable in all three cases. The latent heats of 0.14 and $0.30\ J\ g^{-1}$ for two N^*_{LC}-TGB_C transitions reported in Ref. [14] also correspond very well with the DSC latent heat estimates for the transitions at T_6 that we ascribe to N^*_{LC}-TGB_C (see Table I). It has already been pointed out in Sec. II that the TGB_C-Sm$\tilde{C}$ ΔH_7 latent heat of $\sim 0.05\ J\ g^{-1}$ is comparable to TGB_C-SmC^* values [14].

Evidence about the structure of the low-temperature

smectic-X phase for compounds with $n \geq 14$ is limited in Ref. [16] since it is based on the x-ray powder pattern of the $n=16$ compound at a single temperature plus microscopic textures as a function of temperature for several homologs. Our assignment of this phase as Sm$\tilde{C}$ is largely by analogy with the phase behavior of nonchiral frustrated smectics [3,4]. Note that a Sm$\tilde{C}$ phase can exhibit weak molecular tilt; see Ref. [4] and Fig. 10 in Ref. [3]. Clearly a high-resolution x-ray study is needed to confirm our Sm$\tilde{C}$ assignment and to establish the structures of the TGB$_C$ and N^*_{LC} phases. However, it should be pointed out that the microscopic textures in the SmX phase of Ref. [16] are typical of the Sm$\tilde{C}$ textures reported in Ref. [25]. Moreover, recent x-ray studies of the $n=16$ compound as a function of temperature [26] show that in the temperature range corresponding to the Sm$\tilde{C}$ phase there are two Bragg reflections at $2q_0$ and $q' < 2q_0$. The $q''=2q_0-q'$ peak expected for Sm$\tilde{C}$ should be at a small angle (less than 1°) and thus difficult to resolve with the low-resolution Siemans area detector system used in this work. Two relatively strong diffuse x-ray reflections were also observed in the reentrant nematic phase. Their growth in intensity on approaching the Sm$\tilde{C}$ phase indicates the existence of Sm$\tilde{C}$-like fluctuations in the low-temperature end of the nematic phase (the TGB$_C$ region). Thus, all the currently available information is consistent with our assignment of SmX as Sm$\tilde{C}$.

A final comment should be made about the overall increase in C_p on cooling 15OPBNO$_2$ between T_3 and T_8. In this case, the background slope dC_p/dT is negative (roughly -4×10^{-3} J K^{-2} g^{-1}) rather than positive like 14OPBNO$_2$. (approximately $+6.3\times10^{-3}$) or the TGB$_C$ systems in Ref. [14] (approximately $+3.0\times10^{-3}$). The results in Figs. 2 and 3 were reproducible on several runs taken on two different samples of each compound, but we have no definite explanation of this different 15OPBNO$_2$ behavior. As noted in Sec. II, there are sluggish dynamics below 338 K for 15OPBNO$_2$ suggesting long-range effects. We speculate that this feature might be due to a pretransitional rise in C_p associated with a transition that is preempted by freezing. For example, the Sm$\tilde{C}$-SmC_2 transition in DB$_8$ONO$_2$ +DB$_{10}$ONO$_2$ mixtures exhibits a large inverted Landau C_p peak with the Sm$\tilde{C}$ heat capacity showing an increase on cooling starting $\sim$10 K above the transition [3]. A similar pretransitional increase in the smectic heat capacity also occurs in butyloxybenzlidene octylaniline (4O.8) above the SmA-plastic CrB transition [27]. In the case of 14OPBNO$_2$, freezing preempts the Sm$\tilde{C}$ phase so this feature is not seen.

In summary, the competition between chiral twist and long-core frustrated smectic length scales gives rise to an interesting and rich phase behavior. One first-order transition and several nontransitional thermal features have been established in the nematic phase of 14OPBNO$_2$ and 15OPBNO$_2$. A variety of indirect evidence has been presented for the existence of a TGB phase and chiral line liquids N^*_L as well as two types of N^* twisted nematic phases. A high-resolution x-ray study of well-aligned samples is needed to confirm the proposed phase structures.

ACKNOWLEDGMENTS

The work at MIT was supported in part by the MRSEC program of the National Science Foundation under Award No. DMR-9400334 and that at Warsaw University by Grant No. BST562/29/97. The authors wish to thank T. C. Lubensky for several helpful discussions.

[1] C. W. Garland, *Critical Behavior of Polymorphic Smectic-A Liquid Crystals*, in *Geometry and Thermodynamics: Incommensurate Crystals, Liquid Crystals, and Quasicrystals*, edited by J.-C. Toledano, Vol. 229 of NATO Advanced Study Institute Series B: Physics (Plenum, New York, 1990), pp. 221–254.

[2] K. W. Evans-Lutterodt, J. W. Chung, B. M. Ocko, R. J. Birgeneau, C. Chiang, C. W. Garland, E. Chin, J. Goodby, and N. H. Tinh, Phys. Rev. A **36**, 1387 (1987); J. O. Indekeu, A. N. Berker, C. Chiang, and C. W. Garland, *ibid.* **35**, 1371 (1987).

[3] K. Ema, G. Nounesis, C. W. Garland, and R. Shashidhar, Phys. Rev. A **39**, 2599 (1989).

[4] Y. Shi, G. Nounesis, C. W. Garland, and S. Kumar, Phys. Rev. E **56**, 5575 (1997).

[5] J. Prost and P. Barois, J. Chim. Phys. Phys.-Chim. Biol. **80**, 65 (1983); J. Prost, Adv. Phys. **33**, 1 (1984).

[6] J. F. Marko, J. O. Indekeu, and A. N. Berker, Phys. Rev. A **39**, 4201 (1989).

[7] P. G. deGennes and J. Prost, *The Physics of Liquid Crystals*, 2nd ed. (Oxford University Press, New York, 1993), Chap. 6.

[8] S. R. Renn and T. C. Lubensky, Phys. Rev. A **38**, 2132 (1988); Mol. Cryst. Liq. Cryst. **209**, 349 (1991).

[9] S. R. Renn, Phys. Rev. A **45**, 953 (1992).

[10] R. D. Kamien and T. C. Lubensky, J. Phys. I **3**, 2123 (1994).

[11] A. Bouchta, H. T. Nguyen, M. F. Achard, F. Hardouin, C. Destrade, R. J. Twieg, A. Maaroufi, and N. Isaert, Liq. Cryst. **12**, 575 (1992).

[12] T. Chan, C. W. Garland, and H. T. Nguyen, Phys. Rev. E **52**, 5000 (1995).

[13] H. T. Nguyen, A. Bouchta, L. Navailles, P. Barois, N. Isaert, R. J. Twieg, A. Maaroufi, and C. Destrade, J. Phys. II **2**, 1889 (1992); L. Navailles, R. Pindak, P. Barois, and H. T. Nguyen, Phys. Rev. Lett. **74**, 5224 (1995); A. Bouchta, H. T. Nguyen, L. Navailles, P. Barois, C. Destrade, F. Bougrioua, and N. Isaert, J. Mater. Chem. **5**, 2079 (1995).

[14] L. Navailles, C. W. Garland, and H. T. Nguyen, J. Phys. II **6**, 1243 (1996).

[15] W. Pyzuk, E. Gorecka, J. Mieczkowski, and J. Przedmojski, J. Phys. II **2**, 1465 (1992); W. Pyzuk, E. Gorecka, and J. Mieczkowski, Europhys. Lett. **22**, 371 (1993); E. Gorecka, W. Pyzuk, and J. Mieczkowski, Mol. Cryst. Liq. Cryst. **249**, 33 (1994).

[16] E. Gorecka, J. Mieczkowski, and L. Chen, Liq. Cryst. **23**, 185 (1997).

[17] G. N. Nounesis, S. Kumar, S. Pfeiffer, R. Shashidhar, and C. W. Garland, Phys. Rev. Lett. **73**, 565 (1994).

[18] C. W. Garland, Thermochim. Acta **88**, 127 (1985); K. Ema, T. Uematsu, A. Sugata, and H. Yao, Jpn. J. Appl. Phys., Part 1 **32**, 1846 (1993).

[19] H. Yao, T. Chan, and C. W. Garland, Phys. Rev. E **51**, 4585 (1995).

[20] X. Wen, C. W. Garland, and M. D. Wand, Phys. Rev. A **42**, 6087 (1990); H. Haga and C. W. Garland, Liq. Cryst. **23**, 645 (1997).

[21] Although a SmC_d^* phase has been reported in [16] to exist in a narrow temperature range below the SmA_d phase for the chiral $n=17$ homolog, the thermal behavior at T_2 as well as the optical texture and pitch variation between T_2 and T_3 indicate that the N_ε^* phase cannot be SmC_d^*.

[22] G. S. Iannacchione, S. Qian, M. Wittebrood, and D. Finotello, Mol. Cryst. Liq. Cryst. **302**, 989 (1997); the asymmetry was most apparent for mixtures with higher amounts (11–13%) of chiral component than those shown in this paper.

[23] T. C. Lubensky (private communication).

[24] L. Navailles, H. T. Nguyen, P. Barois, N. Isaert, and P. de-Lord, Liq. Cryst. **20**, 653 (1996).

[25] V. Faye, A. Babeau, F. Placin, H. T. Nguyen, P. Barois, V. Laux, and N. Isaert, Liq. Cryst. **21**, 485 (1996).

[26] E. Gorecka (unpublished).

[27] K. J. Lushington, G. B. Kasting, and C. W. Garland, J. Phys. (France) Lett. **41**, L419 (1980).